PAPER 53 (SESSION V)

Cyclic deformation and fracture characteristics of a low carbon martensitic steel

P. BEARDMORE and C. E. FELTNER
Scientific Laboratory, Ford Motor Company, Dearborn, Michigan, U.S.A.

Summary

The fatigue resistance of low carbon martensite has been investigated as part of a comprehensive program concerned with the effect of metallurgical structure on the fatigue behavior of iron base alloys. Low carbon martensite has a characteristic high dislocation density and properties of the material are a reflection of this transformation induced substructure. Fatigue tests have been made under strain and stress control covering a life range of from 10 to 10^7 cycles. In the low cycle range, under strain control, some cyclic strain hardening always occurred in the first few cycles. This was followed by appreciable cyclic strain softening and the cyclic stress-strain curve was consequently lower than the monotonic stress-strain curve. Shear bands developed gradually in the material and cracks were generally initiated within them. Stage II cracks propagated in a direction perpendicular to the stress axis and followed a path independent of any microstructural feature. Ripples characteristic of ductile metals were observed on the fracture surface indicating that Stage II cracks grew by a blunting and resharpening process.

Introduction

It is well known that one of the important variables in the resistance of a material to fracture under cyclic loading conditions is its metallurgical structure. This includes not only macroscopic structure such as grain size but also the substructure, i.e. the density and distribution of dislocations present prior to testing. The easiest and most commonly used technique of changing the substructure is by cold working by some fairly drastic mechanical processing technique such as swaging. This produces a high density of dislocations in the material frequently in the form of a cell structure. The presence of such a high density of dislocations produces very significant changes in the response of the material to cyclic loading, for example, in addition to affecting the life the material will cyclically soften whereas in the initially annealed state it would cyclically harden. This paper investigates whether the production of a high dislocation density by a different technique produces a similar response to cyclic straining.

There is another important mechanism by which structures containing an increased dislocation density are produced, namely by phase transformations. Indeed, a large class of steels employs a transformation mechanism to produce the desired properties. This class of steels has a martensitic substructure which is a product of the transformation and controls their macroscopic properties. Inevitably the transformation substructure contains a high density of dislocations, the particular density and distribution of which is dependent on the particular transformation mode. Thus, the initial structure of martensitically transformed steels, even in the tempered state, contains an increased dislocation density which would be expected to affect their response to cyclic straining.

One particular type of such substructure in steels is present in low carbon martensite and is typified by maraging steels and certain iron-nickel alloys [1, 2]. The substructure of the low carbon martensites consists of an exceptionally high density of dislocations with a tendency for cell formation and a cell wall alignment along definite crystallographic directions [2]. In the present investigation, an alloy steel with such a structure has been tested under cyclic straining conditions to determine if the response is similar to cold worked materials, i.e. to ascertain if the mechanism of production of a high dislocation density is important since the dislocation distribution may be different depending on the manner of introduction. Although one particular low carbon martensite alloy was used, the results may be considered to apply generally to all alloys of this class of substructure.

Material, specimens and testing methods

The low carbon alloy steel used had a composition (in wt %) of

Fe-2·99Ni-3·00Mo-0·73Mn-0·26Si-0·07Nb-0·034C.

The alloy, which transforms to martensite on air cooling [3], was in the form of a 6 in × 6 in bar in the as-rolled condition with a finish rolling temperature of 900°C. The alloy possesses sufficient hardenability to avoid transformation to a massive ferrite structure during cooling from the rolling temperature as shown in the isothermal transformation diagrams of a similar alloy, Fig. 1, determined by a dilatometric technique [3]. The shear dominated transformation from austenite to martensite occurs at temperatures below the metastable austenite bay and results in a heavily dislocated structure. A typical electron micrograph of the structure of the material showing the high dislocation density and parallel platelet morphology produced during the transformation is shown in Fig. 2.

Three different types of specimen were found necessary to allow determination of the fatigue properties over a wide life range. A gauge section of 0·25 in diameter and 0·3 in long was used for short life-high strain

specimens. For long life, stress control specimens, the gauge section was 0·125 in diameter and 0·3 in long. In the intermediate life range, a gauge section of 0·25 in diameter and 0·5 in long was used to allow more accurate strain control. Flats were machined on two specimens and the gauge section electropolished to allow replication of the surface at various stages of the life.

All the tests were carried out at room temperature in an electro-hydraulic closed loop MTS system. Both strain and stress control were used under a sine wave cycle imposition of tension-compression. Full details of the testing method are described elsewhere [4]. Tensile tests were made on the same machine at a strain rate of 3×10^{-4} sec^{-1}.

Results

Life behavior and cyclic stress-strain response

The life behavior is summarized in Fig. 3 where total strain range $\Delta\epsilon_t$ is plotted against cycles to failure N_f. Also shown in this figure is the plastic strain range at $\frac{1}{2}N_f$ versus cycles to failure. In Fig. 4, the relation between stress amplitude and cycles to failure are plotted for specimens cycled under stress control conditions. These curves must, of course, be considered relative to the tensile properties of the steel; the tensile stress-strain curve is shown in Fig. 5. Also included in Fig. 5 are other relevant mechanical data such as Young's modulus E and the reduction in cross-sectional area at fracture R.A.

Fatigue specimens cycled under strain control were monitored by the frequent recording of hysteresis loops showing the stress-strain relations at different parts of the life. A typical example is shown in Fig. 6. From this data, a cyclic hardening or softening curve can be constructed by plotting the stress required to maintain the imposed strain as a function of cycles. Several such curves are shown in Fig. 7. With this material, a slight initial hardening occurs followed by a gradual, more pronounced, softening. The net effect is a marked softening, indicating that the material behaves as if it had been cold worked prior to testing.

The hysteresis loops (Fig. 6) also provide more data in the form of a cyclic stress-strain curve which is a measure of the steady state cyclic deformation resistance. By plotting the stabilized values of stress amplitude and plastic strain at the half life for each of the specimens tested, the relation between stress and strain is obtained, i.e. the cyclic stress-strain curve, Fig. 8. Also shown in Fig. 8 is the monotonic tensile stress-strain curve. The net softening effect is apparent since the cyclic curve is beneath the monotonic curve. Again this is a characteristic of a cold worked structure indicating that the high dislocation density due to the transformation to martensite reacts similarly to a high dislocation density introduced by cold work.

Several alternative techniques are available for determining the cyclic stress-strain curve [5]. To check the general validity of the curve determined from the individual specimens, the cyclic stress-strain curve was redetermined from a single specimen by the incremental step test [5]. This involves testing a specimen under strain control with a gradually increasing and then decreasing strain amplitude. After a few blocks of these cycles, the material response stabilizes and a continuous recording of the hysteresis loops through such a cycle is shown in Fig. 9. Landgraf *et al.* [5] propose that the locus of the tips of the loops should correspond to the cyclic stress-strain curve. These data are replotted in Fig. 8 to show the excellent agreement between the two techniques for determining the cyclic stress-strain curve.

Surface damage and fractographic observations

Replicas of electropolished surfaces were taken at various stages of life for a specimen cycled in strain control to give a life of 706 cycles and for a specimen cycled in stress control which fractured after 33,010 cycles. A thin film of silver was deposited on the replicas and they were examined in the optical microscope. The crack initiation process appeared to be the same in both cases, namely the gradual development of short, intense shear bands at approximately 45° to the stress axis (see arrow in Fig. 10). Alternatively, the presence of an inclusion can promote crack nucleation, Fig. 11. The shear bands eventually became short cracks and the linking up of these cracks produced severe, 45° cracks on the surface of the specimen, Fig. 12. This was particularly pronounced in the shorter life specimen. For the longer life specimen, the crack initiation process appeared similar but with an appreciably lower density of crack sites for the same percentage of life, Fig. 13. No evidence was found of crack nucleation in prior austenite grain boundaries and crack nucleation, in the absence of inclusions, appears to be exclusively confined to shear bands.

A section through a cracked specimen indicated that the crack initially propagated at a considerable angle to the stress axis before adopting the more usual mode perpendicular to the stress axis, Fig. 14 (a). The major portion of crack propagation occurred perpendicular to the stress axis and appeared to follow a path independent of any particular microstructural feature, Fig. 14 (b). Replicas of the fracture surfaces examined in the electron microscope revealed the well known striations, and examples of both long and short life fractures are shown in Fig. 15.

Discussion

Phenomenological behavior

The alloy responds to cyclic loading in exactly the same manner as cold worked materials as evidenced by cyclic softening, Fig. 7, and the cyclic

stress-strain curve, Fig. 8. The manner in which the high dislocation density is introduced appears to be immaterial as regards the subsequent fatigue behavior. If a high dislocation density already exists prior to cyclic loading, then the process of fatigue presumably consists of the gradual rearrangement of the dislocations into some sort of stable substructure (usually of the cell type) more characteristic of the fatigue process. Since this process involves the localized rearrangement of an alien dislocation structure to one characteristic of the cyclic state a softening of the material can result as this rearrangement takes place. (In the case of an initially annealed structure, the cyclic straining process consists of dislocation multiplication and direct arrangement into a stable structure and must thus always constitute a hardening process.) It seems likely, therefore, that any processing technique which produces a high density of dislocations in a material whether by deformation or transformation will result in cyclic softening due to dislocation rearrangement.

The shape of the monotonic stress-strain curve, Fig. 5, is also similar to that of deformed metals. There is a relatively small amount of uniform elongation(~6%) prior to considerable necking. The 0·2% flow stress of 108,000 lb/in^2 is relatively high in relation to the tensile strength of 146,000 lb/in^2. The presence of the transformation induced substructure can therefore be assessed as having its maximum effect on the yield stress i.e., the 0·2% flow stress. Thus, the yield stress is much higher than for a similar structure of normal low dislocation density. This difference becomes apparent (see below) in comparing the stress for the fatigue strength to the tensile mechanical properties.

A quantity frequently used for comparison of the fatigue data of different materials is the ratio of the fatigue strength (FS) to the tensile strength (TS). From Fig. 4 the minimum fatigue strength of 67,000 lb/in^2 at lives greater than 3×10^6 cycles, gives a ratio FS/TS of 0·46. A ratio of about 0·5 is common for many steels and thus, the fatigue ratio for this alloy is normal [6].

Fatigue data of different materials have also been compared on the basis of the ratio of fatigue strength to yield strength. McEvily and Johnston [7] have compiled such data for annealed metals indicating that for the f.c.c. metals copper and its alloys, aluminum and nickel, the ratio is approximately unity; for b.c.c. iron this ratio is even higher. In the present work, the ratio is considerably less than unity (~0·6) presumably resulting from the yield stress being raised significantly by the transformation substructure. Consequently the flow stress of this material is anomalously high, and a truer comparison would have to be made with cold worked materials. On the other hand, the 'cold working' effect due to the transformation substructure has a much smaller effect on the tensile strength, and therefore the ratio FS/TS is not significantly different from that of other steels.

Empirical methods are available [8] for estimating the fatigue properties of materials from tensile data. One such equation used in this type of estimation can be written: [8]

$$\Delta\epsilon_t = 3{\cdot}5\,\frac{\sigma_u}{E}\cdot N_f^{-0{\cdot}12} + \epsilon_F^{\,0{\cdot}6} N_f^{-0{\cdot}6}$$

where $\Delta\epsilon_t$ is the total strain range, N_f is the number of cycles to failure, σ_u is the tensile strength, ϵ_F is true fracture ductility and E is Young's modulus. The exponents are based on the average values derived from a large number of tests [8]. In Fig. 16, the fatigue resistance of this material based on the empirical equation is compared with the smooth curve for the experimental data from Fig. 3. At short lives, the equation predicts somewhat longer lives than found experimentally. The inverse is true at long lives. The largest discrepancy in using the empiricism to estimate the fatigue resistance of this material would be in the long life region. The greater deviation between experiment and empiricism at long lives is due to the presence of a 'fatigue limit' i.e., a levelling off of the $\Delta\epsilon_t - N_f$ curve at a $\Delta\epsilon_t$ value below which fatigue failure is highly improbable. Since the equation does not account for a fatigue limit, this discrepancy is not unexpected.

Fracture

The well documented concept of fracture under cyclic straining in f.c.c. materials can be used as a model for comparison with fracture in the low carbon martensite alloy used in the present investigation. Fatigue fractures as detailed in f.c.c. structures [9], can be considered to consist of three stages, crack nucleation followed by two separate stages (I and II) of crack propagation. The proportion of the life spent in each of these stages is a function of both the material characteristics and the particular imposed conditions. In general, the process of crack nucleation consists of the generation of a small crack by the concentration of plastic strain in a localized region. Stage I crack propagation is the growth of the crack along well defined shear bands with the crack having a net angle of approximately 45° to the stress axis. This type of crack growth eventually changes to Stage II type propagation perpendicular to the stress axis in which progress of the crack is characterized by well defined striations on the fracture surface marking the points of arrest of the crack. Crack growth in this region consists of a blunting of the crack on the tensile half of the cycle followed by resharpening on the compressive half, leading to a step type of growth pattern.

The crack nucleation process in the present work consisted of the gradual development of pronounced slip bands, Fig. 10. The presence of inclu-

sions could promote this phenomenon, Fig. 11, but the process is still essentially the same. Frequently, a localized series of several short slip bands would form and eventually one of the bands would nucleate a small crack. There was no apparent association between prior austenite grain boundaries and the subsequent formation of these localized shear band cracks.

Crack nucleation seems to be by the same process for the whole range of lives studied. The rate of formation and the intensity of the shear bands are both greater at short lives than long lives but the process is exactly the same in character. One phenomenon much more prevalent in the short life specimens is the formation of a crack along two shear bands at 90° to each other forming a V shaped crack, Fig. 12. This type of crack was not observed in long life specimens. The most significant difference between short and long life specimens was the much higher density of cracks in short life specimens.

In any situation in which intense shear bands are produced, irrespective of the deformation mode (e.g., in the necking region of a ductile material being deformed in tension) the mechanisms are immediately available for the production of cracks at any geometric discontinuity in the structure [10, 11]. For example, the heavy localized shear would produce a void around an inclusion. Consequently, if the product of any deformation is a heavy, localized shear, then the potential of crack nucleation is very great *provided* an inclusion or similar discontinuity is present. (It should be emphasized that even in the presence of heavy shear, a crack cannot form in a completely homogeneous matrix.) The production of a crack by this technique is essentially a mechanism of ductile fracture in that it involves the production of voids at discontinuities and their subsequent coalescence into a macroscopic crack.

In the low carbon martensite investigated, there are numerous sites at which the shearing effect could nucleate cracks. Even though the carbon content is low, there are carbides in the structure and these would be an ideal source of void formation. In addition, the presence of crystallographic discontinuities can also provide suitable sites for void formation. Usually these are of the grain boundary type but the crystallographic changes present in the martensite boundaries may also be capable of acting in a similar manner. It is known from the observations, Fig. 11, that inclusions can act in such a manner but the effect of an inclusion is only an exaggerated example of what is happening through the structure, namely the generation of voids at structural discontinuities due to the intense shear.

Stage I crack growth i.e., growth along shear bands, appears to take place as a surface phenomena as part of the crack nucleation process in the linking of shear band cracks, Fig. 12. It also occurs for a short distance into the specimen, Fig. 14 (a), although the area of Stage I crack

propagation is small compared to the subsequent Stage II propagation perpendicular to the stress axis. The formation of intense shear bands appears, therefore, to be the critical event in cyclic loading of this material. The shear bands are always the sites for the production of cracks and, in addition, can also act as preferred crack propagation paths particularly in short life specimens.

The progress of the crack during Stage II propagation is characterized by ripple formation, Fig. 15. These ripples are a characteristic of fatigue fractures of ductile metals and are strong evidence that the crack grows by a similar mechanism i.e., by a blunting and resharpening process. This growth process is essentially independent of the microstructure as for other materials and appears to be exactly analogous to Stage II growth in other materials [9].

Conclusions

The introduction of a high dislocation density into a material produces similar mechanical responses on cyclic straining independent of the mechanism of introduction of the dislocation structure. Low carbon martensite contains an exceptionally high dislocation density due to the martensite transformation and consequently materials of this structure show a marked cyclic softening effect. The fracture process consists of the gradual development of localized shear bands in which cracks nucleate. The fracture process occurs in a similar manner to that in ductile f.c.c. metals, namely crack nucleation followed by Stage I and Stage II crack propagation. The proportion of crack growth in Stage I is small and the crack growth process occurs by the blunting and resharpening mechanism of Stage II.

Acknowledgements

The authors are grateful to Drs. T. L. Johnston and C. L. Magee for helpful discussions. Thanks are also due to M. R. Mitchell for technical assistance.

References

1. OWEN, W. S., WILSON, E. A. and BELL, T. 'High strength materials', edited by V. F. Zackay, Wiley, New York, 1965, p. 167.
2. SPEICH, G. R. and SWANN, P. R. 'Yield strength and transformation substructure of quenched iron-nickel alloys', *J.I.S.I.*, vol. 203, p. 480, 1965.
3. McEVILY, A. J., DAVIES, R. G., MAGEE, C. L. and JOHNSTON, T. L. 'Transformations and hardenability in steel', published by Climax Molybdenum Corp. of Michigan, 1967, p. 179.
4. FELTNER, C. E. and MITCHELL, M. R. 'Methods of low cycle fatigue testing'. to be published as ASTM STP, 1969.

5. LANDGRAF, R. W., MORROW, J. and ENDO, T. 'Determination of the cyclic stress-strain curve', presented at 70th Annual Meeting Amer. Soc. Testing Mats., Boston, June, 1967, to be published.
6. MOORE, H. F. and JASPER, T. M. 'An Investigation of the fatigue of metals', *Univ. Ill. Eng. Exp. Sta. Bull.*, No. 136, 1923.
7. McEVILY, A. J. and JOHNSTON, T. L. 'The role of cross-slip in brittle fracture and fatigue', First International Conference on Fracture, vol. 2, p. 515, 1965.
8. HALFORD, G. R. and MANSON, S. S. 'Application of a method of estimating high-temperature low-cycle fatigue behaviour of materials', *Trans. ASM*, vol. 61, p. 94, 1968.
9. LAIRD, C. 'Fatigue crack propagation', Am. Soc. Testing Mats., ASTM STP 415, p. 131, 1967.
10. ROGERS, H. C. 'The tensile fracture of ductile metals', *Trans. Met. Soc. AIME*, vol. 218, p. 498, 1960.
11. PUTTICK, K. E. 'Ductile fracture in metals', *Phil. Mag.*, vol. 4, p. 964, 1959.

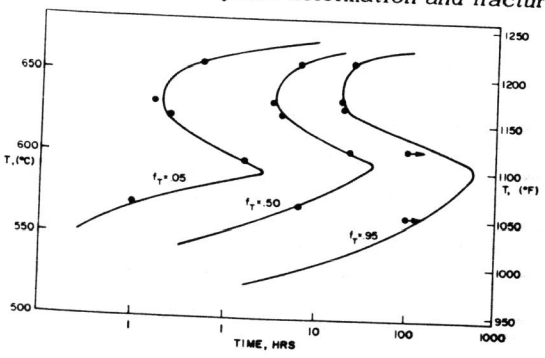

Fig. 1. Isothermal transformation diagram from reference 3. The fraction transformed f_t as a function of time was determined by a dilatometric technique.

Fig. 2. Electron micrograph of the martensitic steel showing the heavily dislocated substructure produced during transformation.

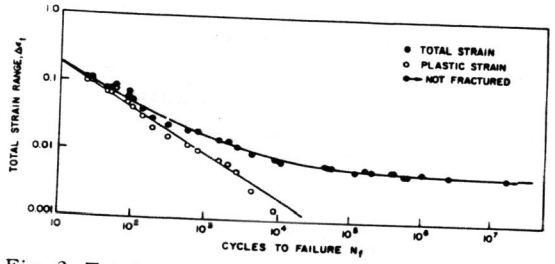

Fig. 3. Total strain range vs. number of cycles to failure.

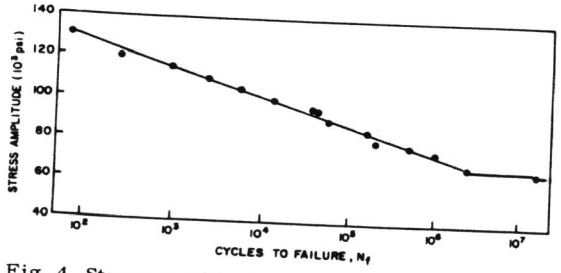

Fig. 4. Stress amplitude vs. number of cycles to failure. All the specimens were cycled in stress control.

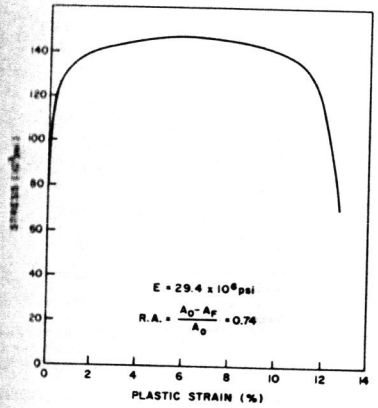

Fig. 5. Tensile stress-strain curve of the steel at room temperature.

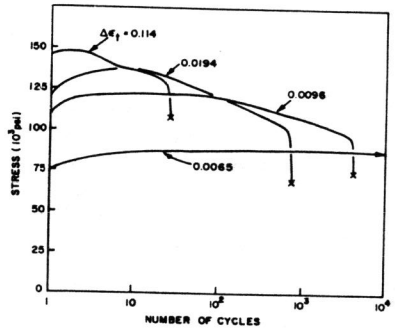

Fig. 7. Stress as a function of number of cycles for specimens tested at different strain ranges.

Fig. 6. Example of the change in the hysteresis loops for a specimen tested under strain control. The loops indicate the changing relation between stress and strain.

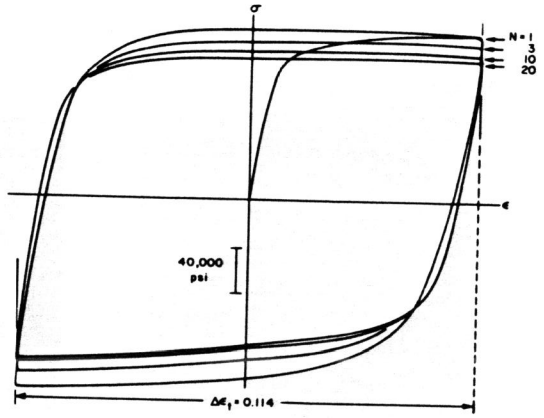

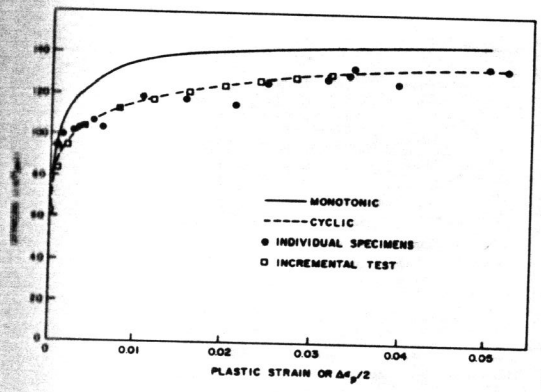

Fig. 8. Cyclic stress-strain curve determined by two different techniques. The monotonic stress-strain curve is included for comparison.

lower dislocation density by annihilation & redistribution cf. cold-worked materials

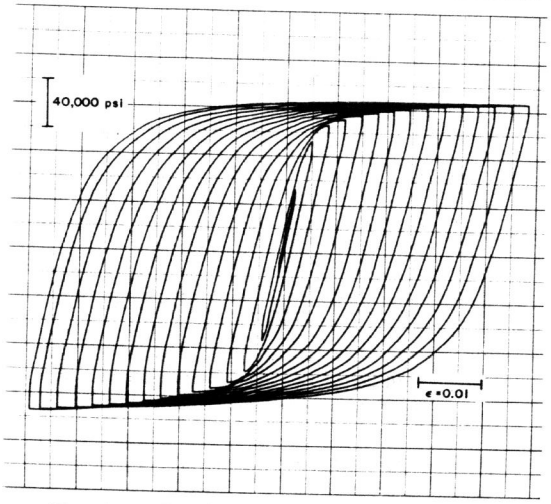

Fig. 9. The hysteresis loops recorded in an incremental step test as the strain was increased.

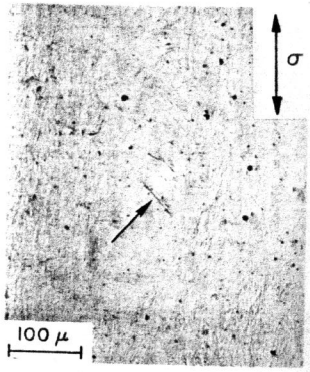

Fig. 10. Development of shear bands after 50 cycles in a specimen cycled in strain control (N_f = 706 cycles).

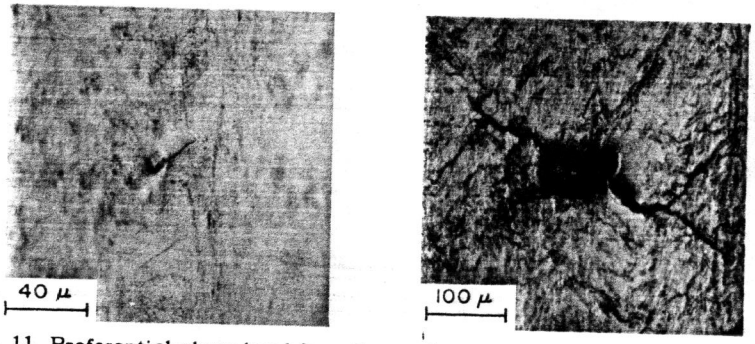

Fig. 11. Preferential shear band formation and crack nucleation around inclusions.

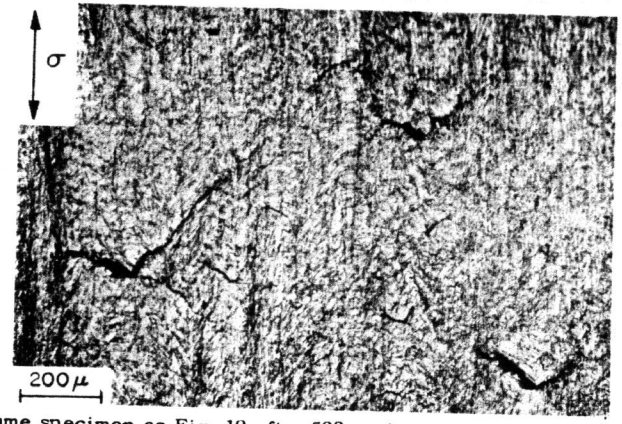

Fig. 12. Same specimen as Fig. 10 after 500 cycles showing the high density and severity of the cracks formed (N_f = 706 cycles).

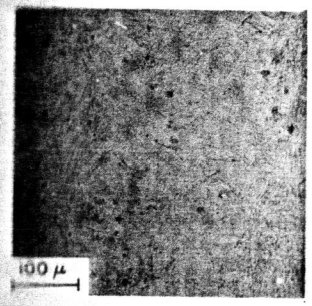

Fig. 13

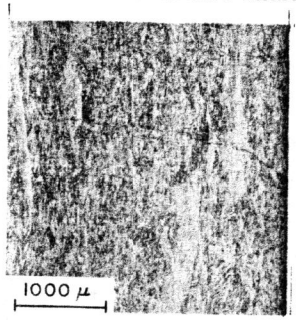

Fig. 14 (a)

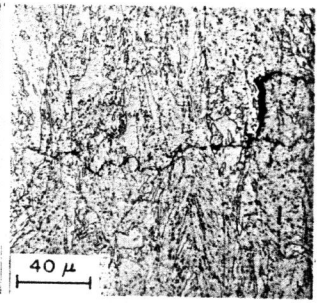

Fig. 14 (b)

Fig. 13. Development of shear bands after 20,000 cycles in a specimen cycled in a stress control which failed after 32,010 cycles.

Fig. 14. Section through a cracked specimen showing (a) the crack initially propagates at a large angle to the stress axis and then perepndicular to the stress axis, and (b) crack propagation perpendicular to the stress axis does not follow any particular microstructural feature.

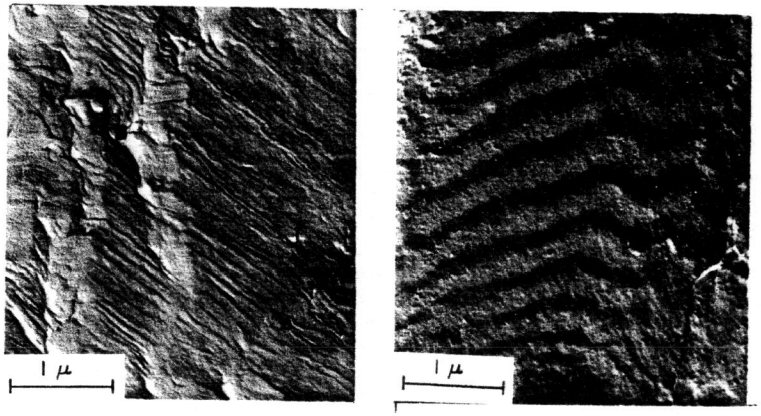

Fig. 15. Replica of the fracture surfaces of specimens which failed after (a) 10,529 cycles, (b) 2,418,480 cycles – showing the characteristic striations of ductile crack growth.

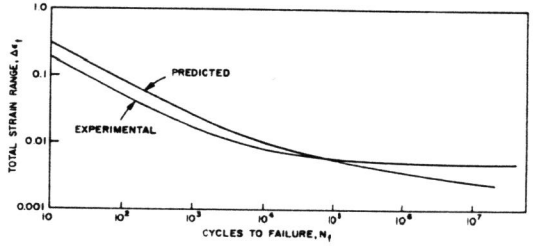

Fig. 16. Comparison of experimental and predicted lives. The experimental data is the smooth curve from Fig. 3.